Review

A Review of the Use of Semiconductors as Catalysts in the Photocatalytic Inactivation of Microorganisms

Elzahraa A. Elgohary [1], Yasser Mahmoud A. Mohamed [1], Hossam A. El Nazer [1], Oussama Baaloudj [2], Mohammed S. S. Alyami [3], Atef El Jery [4], Aymen Amine Assadi [5] and Abdeltif Amrane [5,*]

[1] National Research Centre, Photochemistry Department, Dokki, Giza 12622, Egypt; chemistzahra2000@gmail.com (E.A.E.); y.m.a.mohamed@outlook.com (Y.M.A.M.); dr_hosamnazer@yahoo.com (H.A.E.N.)
[2] Laboratory of Reaction Engineering, USTHB, BP 32, Algiers 16111, Algeria; obaaloudj@gmail.com
[3] Department of Science, King Abdulaziz College of Military, Riyadh 14514, Saudi Arabia; m.ss.ss@hotmail.com
[4] Department of Chemical Engineering, College of Engineering, King Khalid University, Abha 61411, Saudi Arabia; ajery@kku.edu.sa
[5] Ecole Nationale Supérieure de Chimie de Rennes, Universite de Rennes CNRS, ISCR-UMR 6226, F-35000 Rennes, France; aymen.assadi@ensc-rennes.fr
* Correspondence: abdeltif.amrane@univ-rennes1.fr; Tel.: +33-02-2323-4000

Abstract: Obtaining clean and high-quality water free of pathogenic microorganisms is a worldwide challenge. Various techniques have been investigated for achieving an effective removal or inactivation of these pathogenic microorganisms. One of those promising techniques is photocatalysis. In recent years, photocatalytic processes used semiconductors as photocatalysts. They were widely studied as a green and safe technology for water disinfection due to their high efficiency, being non-toxic and inexpensive, and their ability to disinfect a wide range of microorganisms under UV or visible light. In this review, we summarized the inactivation mechanisms of different waterborne pathogenic microorganisms by semiconductor photocatalysts. However, the photocatalytic efficiency of semiconductors photocatalysts, especially titanium dioxide, under visible light is limited and hence needs further improvements. Several strategies have been studied to improve their efficiencies which are briefly discussed in this review. With the developing of nanotechnology, doping with nanomaterials can increase and promote the semiconductor's photocatalytic efficiency, which can enhance the deactivation or damage of a large number of waterborne pathogenic microorganisms. Here, we present an overview of antimicrobial effects for a wide range of nano-photocatalysts, including titanium dioxide-based, other metal-containing, and metal-free photocatalysts. Promising future directions and challenges for materials research in photocatalytic water disinfection are also concluded in this review.

Keywords: photocatalysis; semiconductor; waterborne microorganism; inactivation; nanotechnology

1. Introduction

Water is one of the most vital pillars for sustaining all life forms on our planet. Not only is it essential for drinking and cooking, but it is also required for other purposes such as agriculture, food production, sanitation, industrial processes and ecosystems. Although water covers 71% of the Earth's surface, oceans account for 96.5% of the total surface water but are unsuitable for human consumption [1–4]. While freshwater constitutes about 2.5% of the full hydrosphere water, about 30.1% is present as groundwater, and 68.7% is stored in glaciers and permanent snow cover [5]. This leaves only 1.2% freshwater in swamps, lakes, rivers, soil moisture, and other sources [6]. Technological advances, population growth, agricultural discharge, inappropriate sanitation, water treatment plants, and rapid industrialization cause water pollution, which have adverse effects on human health and the environment [7–9]. Therefore, water pollutants can be classified as biological

(pathogens) or chemical contaminants [10]. Pathogens are microorganisms (such as bacteria, viruses, and protozoa) that can cause or spread various diseases to human beings, plants, or even animals through water [7].

According to the World Health Organization (WHO) 2016 report, it is estimated that about 0.84 million deaths in 2012 were related to water pollution [11]. Water contaminated with pathogenic microorganisms can lead to the spread of numerous diseases (such as hepatitis, malaria, dysentery, cholera, and typhoid fever), which vary in their severity and can be fatal as *Norovirus*, *Echo* viruses, *E. coli*, and *Salmonella* [7,12]. Furthermore, the global public health was threatened by the first Severe Acute Respiratory Syndrome Coronavirus (SARS-CoV-1) outbreak in 2002 followed by the Middle East Respiratory Syndrome Coronavirus (MERS-CoV) and Severe Acute Respiratory Syndrome Coronavirus 2 (SARS-CoV-2, also known as COVID-19 pandemic) outbreaks in 2012 and 2020, respectively [13]. SARS-CoV-1 was reported to exist in hospital wastewater for 2 days and 14 days at 20 °C and 4 °C, respectively. COVID-19 is also RNA positive in hospital wastewater, meaning that these viruses could infect drainage systems. Accordingly, the coronavirus inactivation and disinfection techniques of sewage discharged from hospitals and biomedical laboratories have gained significant attention from the scientific community [14,15].

Obviously, acquiring clean and safe water free of pathogenic microorganisms is a critical global issue for sustaining human health and ecosystems. This can be achieved by removing, inactivating, or killing these pathogens. Therefore, cheap, green, and effective water disinfection or sterilization methods are urgently required [16]. Chlorination, ozone, and ultraviolet irradiation are the traditional technologies used in water/wastewater disinfection. Although the chlorination technique has high efficiency, hazardous mutagenic, and carcinogenic disinfection by-products are generated from the chlorine that reacts with the organic materials present in microorganisms. Some waterborne pathogens are reported to be resistant to chlorine disinfection, such as viruses, specific bacteria as *Legionella*, and *protozoans* as *Cryptosporidium* and *Giardia lamblia cysts*. Unlike chlorination techniques, ozone and ultraviolet irradiation treatments do not leave any residues in treated water/wastewater leading to no water recontamination. However, the high operating costs of the ozone disinfection process, the complexity of its operations, and the production of toxic disinfection by-products such as bromates are the main limitations of this disinfection technique. Despite the low costs of ultraviolet irradiation, it has some drawbacks, including: (i) certain viral types are highly resistant to UV radiation, such as rotaviruses and adenoviruses, and (ii) the inadequate penetration power that inactivates surface wastewater pathogens resulting in regrowth of the treated bacterial cells after irradiation removal [14,16–18]. Accordingly, new techniques are needed to overcome the limitations of the traditional disinfection methods.

Over the last decades, the Advanced Oxidation Processes (AOPs) have been considered efficient environmental remediation techniques. These processes involve hydroxyl radicals and other strong oxidants to eliminate the hazardous organic pollutants efficiently through direct or indirect methods. Due to the high standard potential of these radicals (E° = 2.80 V/SHE), they are classified as one of the strongest oxidizing agents. They can react with a vast range of pollutants producing hydroxylated or dehydrogenated products leading to mineralization (conversion into CO_2, water, and inorganic ions) [19].

Photocatalysis, as one of the AOPs techniques, has greatly attracted the scientific community's concern. In 1985, the photocatalysis technique was used for the first time by Matsunaga and his group as an effective water disinfection process [20], where Pt-loaded TiO_2 photocatalyst deactivated various microorganisms, such as *Lactobacillus acidophilus*, *Saccharomyces cerevisiae*, and *Escherichia coli* [16]. Since then, the photocatalysis technique is widely used in water disinfection because of its high efficiency, low cost, being safe and non-toxic, its ability to disinfect a wide range of microorganisms without hazardous by-products, and ability to inactivate different resistant microbial forms, such as fungal spores and bacterial endospores. In addition, the photocatalyst remains unchanged during reaction leading to less chemical consumption; the photocatalyst can also be used for

multiple cycles without losing its activity and can work at deficient concentrations because the contaminant is strongly attracted to the catalyst surface [21–24].

Based on photocatalytic process technique advantages, heterogeneous photocatalysis using semiconductors is more efficient than conventional methods for contaminant control in water because semiconductors have different convenient properties suitable for the photocatalytic reaction as light absorption properties, ability to produce charge carriers when activated with light photons, and their electronic structure [19,25].

This review provides a concise summary of recent advances in photocatalytic water disinfection, with a focus on bacteria and virus disinfection. The following are the key issues that have been addressed in this review:

(i)   The different water disinfection methods.
(ii)   Semiconductors photocatalytic mechanism.
(iii)   Photocatalytic mechanisms for inactivation of various microorganisms in water and the limitations facing the usage of TiO_2 as photocatalyst.
(iv)   Recent strategies for enhancing the photocatalytic efficiency for water disinfection.

2. Fundamental Mechanism for Photocatalytic Processes

The photocatalytic reaction is initiated when the semiconductor photocatalyst is excited by photons after irradiation by the light source. These photons cause the electrons (e^-) on the surface photocatalyst to become 'excited' in the valance band if the energy of the photons ($E_{h\upsilon}$) is greater than or equal to the bandgap (E_g) [26–28]; this causes the e^- to jump into the conduction band. Once the e^- have absorbed to the conduction band (e_{CB}^-), a positive hole is formed on the valence band (h_{VB}^+), according to the following equation:

$$\text{Photocatalyst} + \text{h}\upsilon \xrightarrow{E_{h\upsilon} \geq E_g} e_{CB}^- + h_{VB}^+ \tag{1}$$
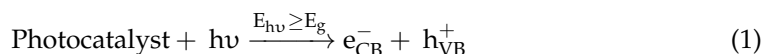
This process lasts for a few femtoseconds and is then followed by recombination of the excited negative electrons in the conduction band (CB) with the previously generated positive holes at the valence band (VB) either on the surface or in the bulk of the particle releasing heat energy [29–31]. Otherwise, these produced charge carriers (e^- and h^+) can migrate to the surface of the photocatalyst and initiate further redox or oxidation reactions with adsorbed or reactant molecules on the surface if they have sufficient time or energy, as illustrated in Figure 1, which is inspired from a previous article [16]. The oxidation potential of the reaction between the holes and the reactant molecules should be higher than that of the valence band. Generally, in an aqueous environment, the positive holes (h^+) can oxidize water adsorbed at the surface producing hydroxyl radicals ($^\bullet$OH), which can oxidize organic pollutants producing carbon dioxide, water, and mineral salts. Otherwise, the excited electrons (e^-) can rapidly reduce the absorbed oxygen on the surface producing superoxide anion radical (O_2^-). This superoxide anion radical can react with (H^+), forming a hydroxyl radical ($^\bullet$OH), which in turn can undergo further oxidation reaction [32–36].
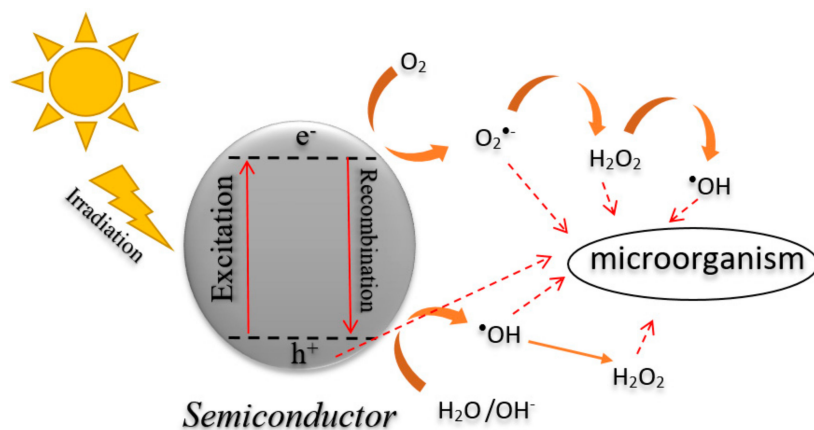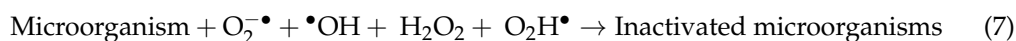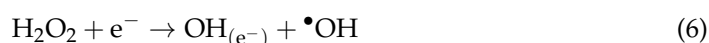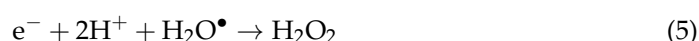

Figure 1. Schematic diagram for the photocatalytic mechanism of a semiconductor.

3. Photocatalytic Water Disinfection

Since about 99 wt% of the pathogenic microorganisms consist of organic compounds, such as proteins, lipids, lipopolysaccharides, polysaccharides, sugars, amino acids, nucleotides, and nucleic acid (DNA and RNA) that can be degraded by photocatalytic materials [37]. The photocatalyst forms reactive oxygen species (ROS), including $^{\bullet}OH$, $O_2^{\bullet-}$, $O_2H^{\bullet}$, and H_2O_2 [38], that have a powerful oxidizing ability for inactivation and/or death of various waterborne pathogenic microorganisms under ambient conditions [18,21]. The ROS can efficiently oxidize the unwanted contaminants present in the water besides water disinfection [39]. This process can be summarized by the next relations (Equations (2)–(7)) [40,41].

$$\text{Semiconductor} + h\upsilon \;\rightarrow\; \text{Semiconductor}^{*} + e^{-} + h^{+} \tag{2}$$

$$O_2 + e^{-} \;\rightarrow\; O_2^{-\bullet} \tag{3}$$

$$H_2O + h^{+} \;\rightarrow\; {}^{\bullet}OH + H^{+} \tag{4}$$

$$e^{-} + 2H^{+} + H_2O^{\bullet} \rightarrow H_2O_2 \tag{5}$$

$$H_2O_2 + e^{-} \rightarrow OH_{(e^{-})} + {}^{\bullet}OH \tag{6}$$

$$\text{Microorganism} + O_2^{-\bullet} + {}^{\bullet}OH + H_2O_2 + O_2H^{\bullet} \rightarrow \text{Inactivated microorganisms} \tag{7}$$

In the case of bacteria, the oxidizing ability of ROS can be achieved by one of three photocatalytic mechanisms that have been proposed in the literature (see Figure 2, which is inspired from an article [21]). In the first mechanism, the cell membrane is attacked by reactive oxygen species (ROS), causing damage to the cell membrane coenzyme A, which inhibits respiration on the cell membrane [40]. This reduces or prevents cellular respiration activity, causing cell lysis [21]. In the second one, the ROS attacks the cell membrane. they enter the bacterial cell causing further oxidation to the internal cellular macromolecular components, such as nucleic acids (as DNA and RNA) and proteins [40]. Eventually, cell lysis occurs. In the last mechanism, the ROS damage the cell membrane and the cell wall; then the internal cellular components (nucleic acids as DNA and RNA, proteins, and some cations) leak out, leading to inactivation and finally to bacterial cell death [21].

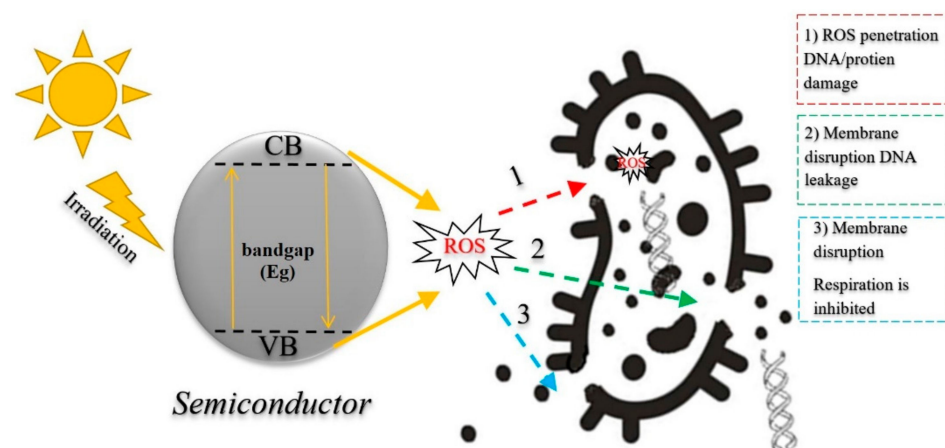**Figure 2.** Proposed photocatalytic water disinfection mechanisms.

4. Photocatalysts Used in Water Disinfection

Based on previous studies, photocatalysis has been used successfully to inactivate various types of bacteria in wastewater. Table 1 summarizes a list of bibliographical references dealing with the implementation of photocatalytic processes using different catalysts for the bacteria inactivation.

Table 1. Semiconductors for bacteria inactivation.

Catalyst	Target Bacteria	Operating Conditions	Inactivation Rate	Ref.
TiO$_2$	*Escherichia coli*	Catalyst dosage: 1.5 g/L; pH: 10; reaction time: 60 min; Initial bacterial cells:10^8 CFU/mL; Temperature: 32 °C; Irradiation: ultraviolet (UV) irradiation at 254 (UV254)	100%	[42]
	Methicillin-resistant Staphylococcus aureus	Fixed TiO$_2$; Reaction time: 10 min; Initial bacterial cells:10^7 CFU/mL; Temperature: 37 °C; Irradiation: ultraviolet (UV)	98.0%	[43]
	Salmonella typhimurium	Catalyst dosage: 100 mg/L; Reaction time: 45 min; Initial bacterial cells: 10^9 CFU/mL; Temperature: 30 °C; Irradiation: ultraviolet (UV)	100%	[44]
	Erwinia amylovora, Xanthomonas arboricola pv. juglandis, Pseudomonas syringae pv. tomato and Allorhizobium vitis.	Catalyst dosage: 0.5 g/L; Reaction time: 30 min; Initial bacterial cells: 10^8 CFU/mL; Temperature: 30 °C; Irradiation: ultraviolet (UV 15 W),	−5 log$_{10}$, −4 log$_{10}$, 100%, 100%, respectively	[45]
ZnO	*Escherichia coli*	Catalyst dosage: 1.5 g/L; pH: 5; reaction time: 180 min; Optical density: 1	94%	[46]
	Coliforms	ZnO film 12.2 mJ/cm^2; Reaction time: 35 min; Initial bacterial cells: 10^7 CFU/mL; Temperature: 82 °C; Turbidity 100 NTU; Irradiation: ultraviolet (UV)	100%	[47]
TiO$_2$ and ZnO	*Saccharomyces cerevisiae, Candida albicans and Aspergillius niger*	Catalyst Dose: 0.01 g/L, Reaction time: 120 min for strains of fungi, 40 min for other strains, Initial bacterial cells: 10^5 CFU/mL, Temperature: 37 °C, Irradiation: ultraviolet (UV)	100%	[48]
Ag/SnO$_2$/ZnO	*Bacillus species*	Catalyst dosage: 500 mg/L; Reaction time: 210 min; Initial bacterial cells: 10^7 CFU/mL; Temperature: 37 °C	100%	[49]
Bi$_2$WO$_6$	*Escherichia coli*	Catalyst dosage: 0.2 g/L; Initial bacterial cells: 2 × 10^6 CFU/mL and light intensity: 48 mW/cm^2; Reaction time: 4 h; Irradiation: visible light.	100%	[50]
Pd-Ag/rGO	*Escherichia coli*	Catalyst dosage: 1 g/L; Initial bacterial cells:10^6 CFU/mL; Reaction time: 120 min; Irradiation: artificial solar simulator (light intensity of ~120,000 Lux)	96%	[51]
NiMoO$_4$	*Methicillin-resistant Staphylococcus aureus*	Catalyst dosage: 5 mg/mL, Reaction time: 360 min, Initial bacterial cells: 10^7 CFU/mL	100%	[38]
Pd-BiFeO$_3$	*Enterococcus faecalis*	Catalyst: 2 wt % Pd/BiFeO$_3$, Dose: 1 g/L, Reaction time: 240 min, Initial bacterial cells: 10^7 CFU/mL Temperature: 37 °C	98%–100%	[52]

Table 1 shows several bacteria strains successfully inactivated by several kinds of photocatalytic materials (TiO$_2$, Ag-TiO$_2$, ZnO, and others), which demonstrate the benefice of the photocatalytic process in the disinfection of water from several types of bacteria. Another observation can be derived from this table, the most widely used semiconductor in the literature is TiO$_2$, due to its effectiveness as it shows complete inactivation of various types of bacteria (*Escherichia coli, methicillin-resistant Staphylococcus aureus,* and *Salmonella*

typhimurium). Because semiconductors have shown to be effective in inactivating bacteria, it is worth looking into how they can be used to inactivate viruses.

In the case of viruses, only a few studies on photocatalytic viral disinfection can be found in the literature. The first viral photocatalytic disinfection was conducted in 1994 using TiO_2 as a photocatalyst for the inactivation of phage MS2 [53]. This work sparked further research into TiO_2 and TiO_2-based photocatalysts' antiviral activity in water and wastewater disinfection and sterilization.

However, viruses have simpler structures than bacteria, as most viruses cover their central genetic material (RNA or DNA) by a protein shell (capsid); they are challenging to be removed due to their small size, unique surface properties, and ability to repair and regrowth under suitable conditions. The ROS oxidative ability can damage the protein shell leading to serious leakage and/or destruction of the virus genes, which results in virus inactivation and/or definite viral death [18,21].

Over the last two decades, there have been many appealing photocatalytic applications for viral disinfection, in which the process led to the inactivation of viruses. Bibliographic references related to studies of photocatalytic processes for the inactivation of viruses are listed in Table 2.

Table 2. Semiconductors for viruses' inactivation.

Catalyst	Target Viruses	Operating Conditions	Inactivation Rate	Ref.
TiO$_2$	*A/H1N1 Influenza virus*	Reaction time: 8 h; Initial viral cells: 1×10^8 TCID$_{50}$/mL; Irradiation: ultraviolet light	4-log$_{10}$ (99%)	[54]
	Bacteriophage f2	Catalyst dose of 25 mg/L; Reaction time: 1 h; Initial viral cells: 5.22 log PFU/g, Irradiation: ultraviolet light	95.79%	[55]
	Bacteriophages (MS2, PRD1, phi-X174, and fr)	Catalyst dosage: 1 g/L; UV dose of 8 mJ/cm^2; pH: 7; initial concentration: 4 log PFU/g	85%, 81%, 94%, and 100%	[56]
	Hepatitis B virus(HBsAg)	Catalyst dosage: 0.5 g/L; pH: 7.2; Reaction time: 4 h, Irradiation: ultraviolet light	97%	[57]
	Norovirus (HuNoV)	Reaction time: 20 min; Initial viral cells: 6.1 log PFU/g, Irradiation: ultraviolet light	2,9 log$_{10}$ 99%	[58]
	Rotavirus (Odelia, SA11), Astrovirus, and Feline calicivirus (FCV)	Reaction time: 24 h; pH: 6, T: 30 °C; Initial viral cells: 3.4–5.19 log TCID$_{50}$; Irradiation: ultraviolet light	1.5–3 log$_{10}$	[59]
Tungsten Trioxide-Based (WO$_3$)	*Coronavirus 2 (SARS-CoV-2)*	Reaction time: 30 min; Initial viral cells:1.7×10^4 PFU/mL	1.5 log$_{10}$ 100%	[60]
Pt-WO$_3$	*Influenza virus* H1N1	The catalyst was used as glass plate; Initial viral cells: $10^{7.0}$ TCID$_{50}$/mL; Temperature (25 °C); Reaction time: 6 h; Irradiation: ultraviolet light	>3.0 log$_{10}$ 99.9%	[61]
Ag−AgI/Al$_2$O$_3$	*human rotavirus (and Shigella dysenteriae and Escherichia coli)*	pH 4.5; Initial viral cells: 10^8 CFU/mL; catalyst dose (0.2 g/L); Temperature (25 °C); Reaction time: less than 1 h	100%	[62]
MIL-125 (Ti)-NH$_2$	*Coronavirus 2 (SARS-CoV-2)*	pH: 6; Reaction time: 30 min; Initial viral cells: 1×10^5 TCID$_{50}$/mL	100 TCID$_{50}$/mL 99%	[63]
O-g-C$_3$N$_4$/HTCC-2	*Adenovirus (HAdV-2)*	Photocatalyst dose of 0.15 g/L; pH: 5, Temperature: 37 °CReaction time: 120 min; Initial viral cells: 10^5 MPN/mL	100%	[64]

Table 2 shows that semiconductors also have excellent photocatalytic performance in the viral disinfection of water besides bacteria. It shows also that lot of viruses such as *A/H1N1 Influenza virus, Bacteriophage f2, Hepatitis B virus, Coronavirus 2 (SARS-CoV-2)*,

Shigella dysenteriae, Escherichia coli, human rotavirus, Adenovirus (HAdV-2), and *Norovirus (HuNoV)* has completely inactivated and disinfected from water by various catalysts, this demonstrates the photocatalytic process' efficacy in the viral disinfection. It can be seen in the tables that Titanium dioxide TiO_2 is the most used and efficient catalyst among those semiconductors, as it shows efficient inactivation for all of *A/H1N1 Influenza virus, Bacteriophages (MS2, PRD1, phi-X174, and fr), Hepatitis B virus (HBsAg), Rotavirus (Odelia, SA11), Astrovirus,* and *Feline calicivirus (FCV)*. As a result, it is critical to concentrate on Titanium dioxide TiO_2 as a topical catalyst for microorganism inactivation and to look for ways to improve its photocatalytic effectiveness for water disinfection.

5. Titanium Dioxide as a Photocatalyst

Among the various semiconductor materials, TiO_2 is the most widely used as a photo-catalyst. This is attributed to its strong oxidizing ability, chemical stability, highly reactive, ease of preparation, abundant, reduced cost, low toxicity, chemical inertness, and long-term photostability [65,66]. In addition, titanium dioxide photocatalysts are widely employed in many research fields, such as organic pollutants degradation and mineralization, selective organic synthesis, solar fuels production as hydrogen and methane, the annihilation of pathogenic microorganisms (as bacteria, fungi, parasites), and utilization in anticancer therapies [67,68].

Titanium dioxide belongs to the transition metal oxides family, which can be extracted from various natural ores present throughout the world. It is a well-known n-type semi-conductor due to the presence of oxygen vacancies in its structure. In TiO_2, the crystalline phase, the composition and the surface states strongly affect the electronic structure and the charge properties. There are three crystalline forms of TiO_2: anatase (tetragonal structure), rutile (tetragonal structure), and brookite (orthorhombic structure). The main building unit consists of a titanium atom surrounded by six oxygen atoms forming a distorted octahedral configuration. The rutile phase is stable at most temperatures and pressures in comparison to the other phases. However, both anatase and brookite phases with particle size greater than 14 nm can turnover to rutile at high temperatures [69,70]. The photocatalytic activity of TiO_2 depends on its present phase. The anatase phase is metastable with a bandgap of 3.2 eV, but it has a more efficient photocatalytic activity compared to the other phases (rutile and brookite). While rutile has a bandgap of about 3.02 eV with high chemical stability but it is less photo-active than anatase. Although brookite is metastable and its bandgap is about 3.4 eV, the experimental data on TiO_2 brookite as a photocatalyst is limited due to its rareness, higher density, and the difficulty of preparation. The high photocatalytic activity of anatase can be attributed to its lower density, its higher electron mobility and the longer lifetime of the photo-activated electrons and holes due to the lower oxygen adsorption and higher hydroxylation degree by electrons and holes, respectively, which reduces the charge carriers' recombination rate in anatase than in the other two phases [71–73].

Unfortunately, natural TiO_2 is activated only by the near-UV photons of the solar spectrum ($\lambda < 390$ nm) due to its wide bandgap. While solar light is made up of only 4% of UV but visible light counts for approximately 42% of solar light [32]. This wide-bandgap hinders its usage in environmental applications. Therefore, increasing the photocatalytic activity of TiO_2 is a challenging issue [74,75].

Various strategies have been used to improve the photocatalytic efficiency of TiO_2 under visible light, which includes the following: (i) Bulk or surface doping with metal ions (using transition or noble metals like Cu, Cr, Fe, Ru, Au, Ag, and Pt) or non-metals (as N, S, C, and F) [66,76–78]; (ii) Composite formation, coupling photocatalyst with different bandgap materials like conjugated carbon as carbon nanotubes, or small bandgap semiconductors such as CdS nanoparticles, or polymeric materials [77,79–81]; and (iii) Sensitization with organic dyes, which involves ionic or covalent bonds formed between photocatalyst surface and dye molecules [82–85].

6. Strategies to Improve the Photocatalytic Activity of Titanium Dioxide

Nanotechnology can provide different solutions for water/wastewater treatment by adding or applying different forms of nanomaterials (such as nanoparticles, nanotubes, nanowires, nanofilms, and quantum dots) to the photocatalyst. This can result in more enhanced efficiency on pathogens disinfection due to their large specific surface area, high activity and an increased degree of functionalization, antipathogenic properties, and ability to deactivate various microorganisms, either photothermally or via photocatalysis by the induced reactive oxygen species (ROS) [86–89]. The high surface area to volume ratio of nanomaterials gives a high contact area for reacting with pathogenic microorganisms [80].

With the development of photocatalytic disinfection techniques, semiconductor nano-photocatalysts showed high efficiency in the deactivation or killing a large number of bacteria, either Gram-positive or negative, filamentous and single-cell fungi, algae, protozoa, *mammalian* viruses, and phages, showing that it can be a promising technology for water and wastewater treatments [21].

The Ag-doped TiO_2 nano-photocatalyst showed the highest bacterial inactivation efficiency compared to Cu and Fe doped TiO_2 and bare TiO_2 when applied on waterborne bacterial pathogens (*Escherichia coli*, *Salmonella enterica*, *Shigellaflexneri,* and *Vibrio cholera*) in real and synthetic wastewater. A 100% disinfection efficiency was achieved without any bacteria regrowth after 60 min and 180 min under UV and solar irradiation, respectively [12]. Additionally, the Ag-loaded TiO_2 nano-photocatalyst caused complete disinfection of the parasitic cysts, *Giardia intestinalis* and *Acanthamoeba castellani*, in water under UV light after 30 min, which is higher than the impact of bare TiO_2. Cell viability tests showed that the cysts cell walls were irreversibly damaged by the photocatalyst ROS and do not regrow again [90]. In another study, the Cu-doped TiO_2 nanofibers exhibited high antiviral activity against bacteriophage f2 and complete inactivation of its host bacteria *E. coli* 285 under visible light [91].

The addition of metal chalcogenides nanoparticles on TiO_2 nanoparticles facilitated the visible light absorption and increased photocatalytic activity under visible irradiation, as mentioned by Nazir and her group [68]. The presence of PbS and CdS quantum dots on P25-TiO_2 to prepare nanocomposites exhibited high antibacterial disinfection activity against *Bacillus subtilis* due to the generation of ROS, which penetrates the bacterial cell membrane leading to membrane lipid oxidation and consequently bacterial inactivation. The highest antibacterial activity was for CdS-Titanium based nanocomposite. This is due to the lethal effect of the Cd atom, which binds to proteins' sulfhydryl groups, causing protein denaturation, membrane damage, and thiol binding, thereby destroying the pathogenic microorganism's protective functions [80].

P25-TiO_2/sodium-Y-zeolite composite prepared via solid-state dispersion method exhibited antibacterial properties against *E. coli* and *S. aureus*. For 20% composite maximum growth reduction of bacterial cells was achieved under sunlight for 1 h at room temperature [92]. While TiO_2/C Heterojunctions (Carbon-doped anatase: brookite (80:20) nano-heterojunction) and Degussa P25 suspension attained a significant increase in photocatalysis and antibacterial properties against S. aureus under polychromatic visible-light and Legionella pneumophila under UV irradiation, respectively [93,94].

The metal-free semiconductor graphite carbon nitride (g-C_3N_4) based photocatalysts showed antibacterial properties. In addition, it was reported that it has antiviral activity as it inactivated the phage MS2 under visible light irradiation. The best disinfection performances were attained after 6 h irradiation with 150 mg/L g-C_3N_4 with no virus regrowth recorded due to the shape distortion and RNA damage by the ROS [21]. While employing $AgVO_3$/g-C_3N_4 and $BiVO_4$ photocatalysts inactivated the *Salmonella* and *E. coli* bacteria, respectively [21]. Additionally, in water disinfection under visible light irradiation, metal-containing photocatalysts such as Ag-AgI/Al_2O_3 and Pt-WO_3 inactivated human rotavirus (type 2 wa) after 40 min and Influenza virus H1N1 after 120 min, respectively [61,62].

Besides, bacterial inactivation, TiO_2 based photocatalysts exhibited antimicrobial properties for various types of fungi *(such as Aspergillusniger, Candida famata, Penicillium citrinum,*

and *Trichoderma asperellum*), protozoa (such as *Cryptosporidium parvum, Giardia* species, *Giardia lamblia,* and *Acanthamoeba castellanii*) and algae (such as *Cladophora, Chroococcus, Oedogonium,* and *Melosira* species) [16].

Furthermore, titanium dioxide-based nano-photocatalysts exhibited antiviral properties for a broad spectrum of viruses, including *Polio* virus1, *Phage* (as MS2, T4, and f2), *Hepatitis* B virus, *Murine norovirus, Human adenovirus* 40, *influenza* viruses (as H9N2, H1N1, H3N2, and H5N2), Herpes simplex virus, and SARS coronaviruses [16,18]. Employing a photocatalytic titanium apatite filter led to an effective inactivation of *SARS-CoV-1* coronavirus (which is a large lipid-enveloped and single-stranded RNA virus) under UV irradiation for 6 h. Indeed, the generated ROS damaged the spike proteins leading to the decrease of the viral infectious capacity with 99.99% inactivation efficiency [89,95]. Due to the genome similarities between *SARS-CoV-1* and *SARS-CoV-2*, this latter can be sensitive and affected by disinfectants, like *SARS-CoV-1*. Thus, titanium dioxide-based photocatalysts might be promising against coronaviruses in water/wastewater treatments [14].

The next table (Table 3) shows the improvements of photocatalytic performance of titania with the different strategies (doping, coupling semiconductors or others) in photocatalytic disinfection applications for both bacteria and viruses.

As can be seen from this table, all improved catalysts have given an almost complete disinfection of water for various types of microorganisms, from bacteria to viruses. This proves the advantage of enhancing the activity of a semiconductor by different strategies such as doping and coupling the catalyst.

Table 3. Improved semiconductors for water disinfection.

Catalyst	Target Bacteria	Operating Conditions	Inactivation Rate	Ref.
TiO_2-Ag	*Mycobacterium kansasii and Mycobacterium avium*	Catalyst: Ti/TiO_2eAg nanotube electrode (5 cm × 5 cm); Reaction time: 240 min; initial bacterial cells: 5×10^8 CFU/mL; Temperature: 35 °C; Irradiation: ultraviolet (UV)	99.9%	[96]
1%Cu-N-TiO_2	*Escherichia coli*	Catalyst dosage: 100 mg/L; Initial cell concentration of 1×10^7 CFU/mL; Irradiation time: 100 min; Irradiation: LED light	100%	[97]
0.1Fe-0.4Zn- TiO_2	*Staphylococcus aureus* and *Escherichia coli*	Catalyst dosage: 1 mg/L; Reaction time: 90 min; Initial bacterial cells: 10^4 CFU/mL; Temperature: 37 °C	100%	[98]
B-Doped TiO_2-CNT	*Escherichia coli*	Catalyst Dose: 2 g/L; Reaction time: 240 min; Initial bacterial cells: 10^6 CFU/mL; Irradiation: ultraviolet (UV)	100%	[99]
Co-doped TiO_2	*Campylobacter jejuni, Salmonella Typhimurium, E. coli, Yersinia enterocolitica, Shewanella putrefaciens, Listeria monocytogenes* and *Staphylococcus aureus*	Catalyst dosage: 500 µg/mL; Initial bacterial cells: 10^6 CFU/mL; Reaction time: 3–6 h; Irradiation: UVA irradiation	100%,100%, ~4 $\log_{10}$, ~3 $\log_{10}$,~5 $\log_{10}$, ~2.5 $\log_{10}$, respectively	[100]
C-doped TiO_2	*Salmonella typhimurium*	Catalyst dosage: 1 g/10 mL; Initial bacterial cells: 3×10^9 CFU/mL; pH 7.4; temperature: 37 °C; Reaction time: 1 h; Irradiation: UV-B lamp 5 mW/cm^2	100%	[101]
Fe^{3+} Doped TiO_2/3S$_n$O$_2$	*Salmonella typhimurium*	Catalyst dosage: 250 mg/L, reaction time: 60 min, Initial bacterial cells: 10^6 CFU/mL, Temperature: 37 °C	100%	[102]

Table 3. *Cont.*

Catalyst	Target Viruses	Operating Conditions	Inactivation Rate	Ref.
N-doped TiO_2-coated Al_2O_3	*MS2 bacteriophage*	In the presence of 120 mg L^{-1} Ca^{2+}; Reaction time: 120 min; pH: 6; Initial viral cells: 10^{11} PFU/mL	$4.9 \log_{10}$ (99.99%)	[103]
TiO_2-coated ceramic	Aerosol-Associated *Influenza*	Reaction time: 30 min; Initial viral cells: 10^5 PFU/mL	99%	[104]
Cu-doped TiO_2	*Norovirus (HuNoV)*	UVA-LED wavelength: 365 nm; Cu:TiO_2 ratio: 5.5; Reaction time: 60 min; Initial viral cells: 6.7 log PFU/g	$2.89 \log_{10}$ 99%	[105]

7. Conclusions and Outlook

Considering the fact that waterborne pathogenic microorganisms can threaten human health, their removal or inactivation in water/wastewater is an essential concern for sustainable human life. The photocatalysis technique using semiconductors offers a practical and sustainable strategy for dealing with this problem. Accordingly, semiconductors photocatalytic water disinfection has received great attention recently. TiO_2 is the widest semiconductor used as a photocatalyst due to its strong oxidizing ability, chemical stability, high reactivity, ease of preparation, abundance, cheap, non-toxic, and long-term photostability. Many photocatalysts, especially TiO_2-based, are reported in the literature that can be used in water disinfection. However, their photocatalytic efficiencies are limited under visible light, which reduces their practical applications. Many approaches have been documented to narrow the bandgap, including doping with metal or non-metals, composite formation, coupling with different bandgap materials like carbon nanotubes, or small band-gap semiconductors like CdS nanoparticles, or sensitization, with organic dyes. In addition, nanomaterials can inspire the future development of antimicrobial semiconductor photocatalysts due to their high surface area that increases the contact area available for the reaction between the microorganism and the photocatalyst. Therefore, doping with noble metals nanoparticles is reported to increase the absorption under visible light due to their unique optical properties. As well, metal-free nano-photocatalysts, such as graphite carbon nitride (g-C_3N_4) based photocatalysts, showed antiviral and antibacterial activities under visible light. While the inactivation of bacteria by photocatalysts has been extensively studied in the literature, viral inactivation by photocatalysts has received less attention. Thus, viral photocatalytic disinfection is required to be explored more. Furthermore, future work should focus on understanding the mechanisms of microorganisms' inactivation by photocatalytic materials using computer simulation.

Generally, designing and synthesizing reliable nano-photocatalysts for solar water disinfection need further improvements, especially those based on metal oxides, sulfides, semiconductors, metal-free, graphene, and natural mineral photocatalysts. All the above directions can offer both challenges and future opportunities for more research in photocatalysis and water disinfection.

References

1. Davis, M.L. *Water and Wastewater Engineering*; McGraw-Hill: New York, NY, USA, 2003; ISBN 9780071713856.
2. Alley, E.R. *Water Quality Control Handbook*; McGraw-Hill: New York, NY, USA, 2007; Volume 1, ISBN 0071508708.
3. Bourkeb, K.; Baaloudj, O. Facile electrodeposition of ZnO on graphitic substrate for photocatalytic application: Degradation of antibiotic in a continuous stirred-tank reactor. *J. Solid State Electrochem.* **2021**. [CrossRef]
4. Asadi-Ghalhari, M.; Mostafaloo, R.; Ghafouri, N.; Kishipour, A.; Usei, S.; Baaloudj, O. Removal of Cefixime from aqueous solutions via proxy electrocoagulation: Modeling and optimization by response surface methodology. *React. Kinet. Mech. Catal.* **2021**, *134*, 459–471. [CrossRef]
5. Baaloudj, O.; Nasrallah, N.; Kebir, M.; Khezami, L.; Amrane, A.; Assadi, A.A. A comparative study of ceramic nanoparticles synthesized for antibiotic removal: Catalysis characterization and photocatalytic performance modeling. *Environ. Sci. Pollut. Res.* **2020**, *28*, 13900–13912. [CrossRef]
6. German Advisory Council on Global Change. The freshwater crisis: Basic elements. In *Ways towards Sustainable Management of Freshwater Resources: Annual Report 1997*; Springer: Berlin/Heidelberg, Germany, 1999.
7. Khan, S.T.; Malik, A. Engineered nanomaterials for water decontamination and purification: From lab to products. *J. Hazard. Mater.* **2019**, *363*, 295–308. [CrossRef] [PubMed]
8. Subramaniam, M. *Contesting Water Rights*; Palgrave Macmillan: New York, NY, USA, 2018; ISBN 9783319746265.
9. Benrighi, Y.; Nasrallah, N.; Chaabane, T.; Sivasankar, V.; Darchen, A.; Baaloudj, O. Photocatalytic performances of ZnCr2O4 nanoparticles for cephalosporins removal: Structural, optical and electrochemical properties. *Opt. Mater.* **2021**, *115*, 111035. [CrossRef]
10. Baaloudj, O.; Nasrallah, N.; Kebir, M.; Guedioura, B.; Amrane, A.; Nguyen-Tri, P.; Nanda, S.; Assadi, A.A. Artificial neural network modeling of cefixime photodegradation by synthesized CoBi2O4 nanoparticles. *Environ. Sci. Pollut. Res.* **2020**, *28*, 15436–15452. [CrossRef]
11. Landrigan, P.J.; Fuller, R.; Acosta, N.J.R.; Adeyi, O.; Arnold, R.; Basu, N.; Baldé, A.B.; Bertollini, R.; Bose-O'Reilly, S.; Boufford, J.I.; et al. The Lancet Commission on pollution and health. *Lancet* **2018**, *391*, 462–512. [CrossRef]
12. Mecha, A.C.; Onyango, M.S.; Ochieng, A.; Momba, M.N.B. UV and solar photocatalytic disinfection of municipal wastewater: Inactivation, reactivation and regrowth of bacterial pathogens. *Int. J. Environ. Sci. Technol.* **2019**, *16*, 3687–3696. [CrossRef]
13. Assadi, I.; Guesmi, A.; Baaloudj, O.; Zeghioud, H.; Elfalleh, W.; Benhammadi, N. Review on inactivation of airborne viruses using non—Thermal plasma technologies: From MS2 to coronavirus. *Environ. Sci. Pollut. Res.* **2021**, *2021*, 1–13. [CrossRef]
14. Wang, J.; Shen, J.; Ye, D.; Yan, X.; Zhang, Y.; Yang, W.; Li, X.; Wang, J.; Zhang, L.; Pan, L. Disinfection technology of hospital wastes and wastewater: Suggestions for disinfection strategy during coronavirus Disease 2019 (COVID-19) pandemic in China. *Environ. Pollut.* **2020**, *262*, 114665. [CrossRef]
15. Wang, X.W.; Li, J.S.; Jin, M.; Zhen, B.; Kong, Q.X.; Song, N.; Xiao, W.J.; Yin, J.; Wei, W.; Wang, G.J.; et al. Study on the resistance of severe acute respiratory syndrome-associated coronavirus. *J. Virol. Methods* **2005**, *126*, 171–177. [CrossRef]
16. An, T.; Zhao, H.J.; Wong, P.K. *Advances in Photocatalytic Disinfection*; Springer: Berlin, Germany, 2017; ISBN 978-3-662-53494-6.
17. Zhang, Z.; Gamage, J. Applications of photocatalytic disinfection. *Int. J. Photoenergy* **2010**, *2010*, 764870. [CrossRef]
18. Zhang, C.; Li, Y.; Shuai, D.; Shen, Y.; Wang, D. Progress and challenges in photocatalytic disinfection of waterborne Viruses: A review to fill current knowledge gaps. *Chem. Eng. J.* **2019**, *355*, 399–415. [CrossRef]
19. Akerdi, A.G.; Bahrami, S.H. Application of heterogeneous nano-semiconductors for photocatalytic advanced oxidation of organic compounds: A review. *J. Environ. Chem. Eng.* **2019**, *7*, 103283. [CrossRef]
20. Matsunaga, T.; Tomoda, R.; Nakajima, T.; Wake, H. Photoelectrochemical sterilization of microbial cells by semiconductor powders. *FEMS Microbiol. Lett.* **1985**, *29*, 211–214. [CrossRef]
21. Deng, Y.; Li, Z.; Tang, R.; Ouyang, K.; Liao, C.; Fang, Y.; Ding, C.; Yang, L.; Su, L.; Gong, D. What will happen when microorganisms "meet" photocatalysts and photocatalysis? *Environ. Sci. Nano* **2020**, *7*, 702–723. [CrossRef]
22. Ibhadon, A.O.; Fitzpatrick, P. Heterogeneous photocatalysis: Recent advances and applications. *Catalysts* **2013**, *3*, 189–218. [CrossRef]
23. Islam, M.T.; Jing, H.; Yang, T.; Zubia, E.; Goos, A.G.; Bernal, R.A.; Botez, C.E.; Narayan, M.; Chan, C.K.; Noveron, J.C. Fullerene stabilized gold nanoparticles supported on titanium dioxide for enhanced photocatalytic degradation of methyl orange and catalytic reduction of 4-nitrophenol. *J. Environ. Chem. Eng.* **2018**, *6*, 3827–3836. [CrossRef]
24. Taheri, F.; Amini, A.; Kouhsari, E.; Kiaei, M.R.; Movaseghi, R.; Niknejad, F. Photocatalytic inactivation of microorganisms in water under ultraviolet C irradiation and TiO$_2$. *Rev. Med. Microbiol.* **2020**, *31*, 79–85. [CrossRef]
25. Kenfoud, H.; Nasrallah, N.; Baaloudj, O.; Meziani, D.; Chaabane, T.; Trari, M. Photocatalytic reduction of Cr(VI) onto the spinel CaFe2O4 nanoparticles. *Optik* **2020**, *223*, 165610. [CrossRef]
26. Kenfoud, H.; Baaloudj, O.; Nasrallah, N.; Bagtache, R. Structural and electrochemical characterizations of Bi 12 CoO 20 sillenite crystals: Degradation and reduction of organic and inorganic pollutants. *J. Mater. Sci. Mater. Electron.* **2021**, *32*, 16411–16420. [CrossRef]
27. Baaloudj, O.; Nasrallah, N.; Kenfoud, H.; Algethami, F.; Modwi, A.; Guesmi, A.; Assadi, A.A.; Khezami, L. Application of Bi12ZnO20 Sillenite as an Efficient Photocatalyst for Wastewater Treatment: Removal of Both Organic and Inorganic Compounds. *Materials* **2021**, *14*, 5409. [CrossRef]
28. Baaloudj, O.; Nasrallah, N.; Assadi, A.A. Facile synthesis, structural and optical characterizations of Bi12ZnO20 sillenite crystals: Application for Cefuroxime removal from wastewater. *Mater. Lett.* **2021**, *304*, 130658. [CrossRef]

29. Kenfoud, H.; Nasrallah, N.; Baaloudj, O.; Derridj, F.; Trari, M. Enhanced photocatalytic reduction of Cr(VI) by the novel hetero-system BaFe2O4/SnO2. *J. Phys. Chem. Solids* **2022**, *160*, 110315. [CrossRef]

30. Brahimi, B.; Mekatel, E.; Mellal, M.; Baaloudj, O.; Brahimi, R.; Hemmi, A.; Trari, M.; Belmedani, M. Enhanced photodegradation of acid orange 61 by the novel hetero-junction CoFe$_2$O$_4$/AgCl. *Opt. Mater.* **2021**, *121*, 111576. [CrossRef]

31. Baaloudj, O.; Assadi, A.A.; Azizi, M.; Kenfoud, H.; Trari, M.; Amrane, A.; Assadi, A.A.; Nasrallah, N. Synthesis and Characterization of ZnBi2O4 Nanoparticles: Photocatalytic Performance for Antibiotic Removal under Different Light Sources. *Appl. Sci.* **2021**, *11*, 3975. [CrossRef]

32. Byrne, C.; Subramanian, G.; Pillai, S.C. Recent advances in photocatalysis for environmental applications. *J. Environ. Chem. Eng.* **2018**, *6*, 3531–3555. [CrossRef]

33. Chauhan, A.; Rastogi, M.; Scheier, P.; Bowen, C.; Kumar, R.V.; Vaish, R. Janus nanostructures for heterogeneous photocatalysis. *Appl. Phys. Rev.* **2018**, *5*, 041111. [CrossRef]

34. Chen, Y.; Wang, K.; Lou, L. Photodegradation of dye pollutants on silica gel supported TiO2 particles under visible light irradiation. *J. Photochem. Photobiol. A Chem.* **2004**, *163*, 281–287. [CrossRef]

35. Chiron, S.; Fernandez-Alba, A.; Rodriguez, A.; Garcia-Calvo, E. Pesticide chemical oxidation: State-of-the-art. *Water Res.* **2000**, *34*, 366–377. [CrossRef]

36. Muniandy, L.; Adam, F.; Mohamed, A.R.; Ng, E.P.; Rahman, N.R.A. Carbon modified anatase TiO$_2$ for the rapid photo degradation of methylene blue: A comparative study. *Surf. Interfaces* **2016**, *5*, 19–29. [CrossRef]

37. Ren, H.; Koshy, P.; Chen, W.F.; Qi, S.; Sorrell, C.C. Photocatalytic materials and technologies for air purification. *J. Hazard. Mater.* **2017**, *325*, 340–366. [CrossRef]

38. Ray, S.K.; Dhakal, D.; Regmi, C.; Yamaguchui, T.; Lee, S.W. Inactivation of Staphylococcus aureus in visible light by morphology tuned α-NiMoO4. *J. Photochem. Photobiol. A Chem.* **2018**, *350*, 59–68. [CrossRef]

39. Thandu, M.; Comuzzi, C.; Goi, D. Phototreatment of water by organic photosensitizers and comparison with inorganic semiconductors. *Int. J. Photoenergy* **2015**, *2015*, 10–12. [CrossRef]

40. Baaloudj, O.; Assadi, I.; Nasrallah, N.; El, A.; Khezami, L. Simultaneous removal of antibiotics and inactivation of antibiotic-resistant bacteria by photocatalysis: A review. *J. Water Process Eng.* **2021**, *42*, 102089. [CrossRef]

41. Bono, N.; Ponti, F.; Punta, C.; Candiani, G. Effect of UV irradiation and TiO$_2$-photocatalysis on airborne bacteria and viruses: An overview. *Materials* **2021**, *14*, 1075. [CrossRef] [PubMed]

42. De Vietro, N.; Tursi, A.; Beneduci, A.; Chidichimo, F.; Milella, A.; Fracassi, F.; Chatzisymeon, E.; Chidichimo, G. Photocatalytic inactivation of Escherichia coli bacteria in water using low pressure plasma deposited TiO$_2$ cellulose fabric. *Photochem. Photobiol. Sci.* **2019**, *18*, 2248–2258. [CrossRef] [PubMed]

43. Chen, C.Y.; Wu, L.C.; Chen, H.Y.; Chung, Y.C. Inactivation of staphylococcus aureus and escherichia coli in water using photocatalysis with fixed TiO$_2$. *Water. Air. Soil Pollut.* **2010**, *212*, 231–238. [CrossRef]

44. Fiorentino, A.; Rizzo, L.; Guilloteau, H.; Bellanger, X.; Merlin, C. Comparing TiO$_2$ photocatalysis and UV-C radiation for inactivation and mutant formation of Salmonella typhimurium TA102. *Environ. Sci. Pollut. Res.* **2017**, *24*, 1871–1879. [CrossRef]

45. Kőrösi, L.; Pertics, B.; Schneider, G.; Bognár, B.; Kovács, J.; Meynen, V.; Scarpellini, A.; Pasquale, L.; Prato, M. Photocatalytic inactivation of plant pathogenic bacteria using TiO$_2$ nanoparticles prepared hydrothermally. *Nanomaterials* **2020**, *10*, 1730. [CrossRef]

46. Hwangbo, M.; Claycomb, E.C.; Liu, Y.; Alivio, T.E.G.; Banerjee, S.; Chu, K.H. Effectiveness of zinc oxide-assisted photocatalysis for concerned constituents in reclaimed wastewater: 1,4-Dioxane, trihalomethanes, antibiotics, antibiotic resistant bacteria (ARB), and antibiotic resistance genes (ARGs). *Sci. Total Environ.* **2019**, *649*, 1189–1197. [CrossRef] [PubMed]

47. Yazdanbakhsh, A.; Rahmani, K.; Rahmani, H.; Sarafraz, M.; Tahmasebizadeh, M.; Rahmani, A. Inactivation of Fecal coliforms during solar and photocatalytic disinfection by zinc oxide (ZnO) nanoparticles in compound parabolic concentrators (CPCs). *Asian J. Chem.* **2016**, *27*, 4120–4124. [CrossRef]

48. Seven, O.; Dindar, B.; Aydemir, S.; Metin, D.; Ozinel, M.A.; Icli, S. Solar photocalytic disinfection of a group of bacteria and fungi aqueous suspensions with TiO$_2$, ZnO and sahara desert dust. *J. Photochem. Photobiol. A Chem.* **2004**, *165*, 103–107. [CrossRef]

49. Das, S.; Misra, A.J.; Habeeb Rahman, A.P.; Das, B.; Jayabalan, R.; Tamhankar, A.J.; Mishra, A.; Lundborg, C.S.; Tripathy, S.K. Ag@SnO2@ZnO core-shell nanocomposites assisted solar-photocatalysis downregulates multidrug resistance in Bacillus sp.: A catalytic approach to impede antibiotic resistance. *Appl. Catal. B Environ.* **2019**, *259*, 118065. [CrossRef]

50. Karbasi, M.; Karimzadeh, F.; Raeissi, K.; Rtimi, S.; Kiwi, J.; Giannakis, S.; Pulgarin, C. Insights into the photocatalytic bacterial inactivation by flower-like Bi2WO6 under solar or visible light, through in situ monitoring and determination of reactive oxygen species (ROS). *Water* **2020**, *12*, 1099. [CrossRef]

51. Mallikarjuna, K.; Nasif, O.; Alharbi, S.A.; Chinni, S.V.; Reddy, L.V.; Reddy, M.R.V.; Sreeramanan, S. Phytogenic synthesis of Pd-Ag/rGO nanostructures using stevia leaf extract for photocatalytic H2 production and antibacterial studies. *Biomolecules* **2021**, *11*, 190. [CrossRef]

52. Jaffari, Z.H.; Lam, S.M.; Sin, J.C.; Zeng, H.; Mohamed, A.R. Magnetically recoverable Pd-loaded BiFeO3 microcomposite with enhanced visible light photocatalytic performance for pollutant, bacterial and fungal elimination. *Sep. Purif. Technol.* **2020**, *236*, 116195. [CrossRef]

53. Sjogren, J.C.; Sierka, R.A. Inactivation of phage MS2 by iron-aided titanium dioxide photocatalysis. *Appl. Environ. Microbiol.* **1994**, *60*, 344–347. [CrossRef]

54. Nakano, R.; Ishiguro, H.; Yao, Y.; Kajioka, J.; Fujishima, A.; Sunada, K. Photocatalytic inactivation of in fluenza virus by titanium dioxide thin film. *Photochem. Photobiol. Sci.* **2012**, *11*, 1293–1298. [CrossRef]

55. Zheng, X.; Wang, Q.; Chen, L.; Wang, J.; Cheng, R. Photocatalytic membrane reactor (PMR) for virus removal in water: Performance and mechanisms Photocatalytic membrane reactor (PMR) for virus removal in water: Performance and mechanisms. *Chem. Eng. J.* **2015**, *277*, 124–129. [CrossRef]

56. Gerrity, D.; Ryu, H.; Crittenden, J.; Abbaszadegan, M. Photocatalytic inactivation of viruses using titanium dioxide nanoparticles and low-pressure UV light. *J. Environ. Sci. Heal.-Part A Toxic/Hazardous Subst. Environ. Eng.* **2008**, *43*, 1261–1270. [CrossRef] [PubMed]

57. Zan, L. Photocatalysis effect of nanometer TiO₂ and TiO₂ -coated ceramic plate on Hepatitis B virus. *J. Photochem. Photobiol. B Biol.* **2007**, *86*, 165–169. [CrossRef]

58. Kim, S.; Shahbaz, H.M.; Park, D.; Chun, S.; Lee, W.; Oh, J.; Lee, D.; Park, J. A combined treatment of UV-assisted TiO₂ photocatalysis and high hydrostatic pressure to inactivate internalized murine norovirus. *Innov. Food Sci. Emerg. Technol.* **2017**, *39*, 188–196. [CrossRef]

59. Maneekarn, N. Photocatalytic Inactivation of Diarrheal Viruses by Visible-Light-Catalytic Titanium Dioxide. *Clin. Lab.* **2007**, *53*, 2007–2008.

60. Ghezzi, S.; Pagani, I.; Poli, G.; Perboni, S.; Vicenzi, E. Rapid Inactivation of Severe Acute Respiratory Syndrome Coronavirus 2 (SARS-CoV-2) by Tungsten Trioxide-Based (WO₃) Photocatalysis. *bioRxiv* **2020**, *2*, 1–12.

61. Takehara, K.; Yamazaki, K.; Miyazaki, M.; Yamada, Y.; Ruenphet, S.; Jahangir, A.; Shoham, D.; Okamura, M.; Nakamura, M. Inactivation of avian influenza virus H1N1 by photocatalyst under visible light irradiation. *Virus Res.* **2010**, *151*, 102–103. [CrossRef]

62. Hu, X.; Hu, C.; Peng, T.; Zhou, X.; Qu, J. Plasmon-induced inactivation of enteric pathogenic microorganisms with Ag-AgI/Al2O3 under visible-light irradiation. *Environ. Sci. Technol.* **2010**, *44*, 7058–7062. [CrossRef]

63. Ornstein, A.J.; Ozdemir, R.O.K.; Boehme, A.; Nouar, F. SARS-CoV-2 Inactivation Potential of Metal Organic Framework Induced Photocatalysis. *medRxiv* **2020**, 1–8. [CrossRef]

64. Zhang, C.; Zhang, M.; Li, Y.; Shuai, D. Visible-light-driven Photocatalytic Disinfection of Human Adenovirus by a Novel Heterostructure of Oxygen-doped Graphitic Carbon Nitride and Hydrothermal Carbonation Carbon Applied Catalysis B: Environmental Visible-light-driven photocatalytic disinfecti. *Appl. Catal. B Environ.* **2019**, *248*, 11–21. [CrossRef]

65. Lee, K.; Yoon, H.; Ahn, C.; Park, J.; Jeon, S. Strategies to improve the photocatalytic activity of TiO₂: 3D nanostructuring and heterostructuring with graphitic carbon nanomaterials. *Nanoscale* **2019**, *11*, 7025–7040. [CrossRef]

66. Patil, S.B.; Basavarajappa, P.S.; Ganganagappa, N.; Jyothi, M.S.; Raghu, A.V.; Reddy, K.R. Recent advances in non-metals-doped TiO₂ nanostructured photocatalysts for visible-light driven hydrogen production, CO2 reduction and air purification. *Int. J. Hydrogen Energy* **2019**, *44*, 13022–13039. [CrossRef]

67. Cao, S.; Low, J.; Yu, J.; Jaroniec, M. Polymeric Photocatalysts Based on Graphitic Carbon Nitride. *Adv. Mater.* **2015**, *27*, 2150–2176. [CrossRef] [PubMed]

68. Rodríguez-González, V.; Obregón, S.; Patrón-Soberano, O.A.; Terashima, C.; Fujishima, A. An approach to the photocatalytic mechanism in the TiO₂-nanomaterials microorganism interface for the control of infectious processes. *Appl. Catal. B Environ.* **2020**, *270*, 118853. [CrossRef]

69. Nouri, L.; Hemidouche, S.; Boudjemaa, A.; Kaouah, F.; Sadaoui, Z.; Bachari, K. Elaboration and characterization of photobiocomposite beads, based on titanium (IV) oxide and sodium alginate biopolymer, for basic blue 41 adsorption/photocatalytic degradation. *Int. J. Biol. Macromol.* **2020**, *151*, 66–84. [CrossRef] [PubMed]

70. Khataee, A.; Mansoori, G. Properties of Titanium Dioxide and Its Nanoparticles. In *Nanostructured Titanium Dioxide Materials*; World Scientific Publishing Co. Pte. Ltd.: Singapore, 2011; pp. 5–11.

71. Alotaibi, A.; Sathasivam, S.; Williamson, B.; Kafizas, A.; Sotelo-Vazquez, C.; Taylor, A.; Scanlon, D.; Parkin, I. Chemical Vapor Deposition of Photocatalytically Active Pure Brookite TiO₂ Thin Films. *Chem. Mater.* **2018**, *30*, 1353–1361. [CrossRef]

72. Gupta, S.M.; Tripathi, M. A review of TiO₂ nanoparticles. *Chin. Sci. Bull.* **2011**, *56*, 1639–1657. [CrossRef]

73. Zhang, J.; Zhou, P.; Liu, J.; Yu, J. New understanding of the difference of photocatalytic activity among anatase, rutile and brookite TiO₂. *Phys. Chem. Chem. Phys.* **2014**, *16*, 20382–20386. [CrossRef]

74. El Nazer, H.A.; Salman, S.A.; Elnazer, A.A. Irrigation water quality assessment and a new approach to its treatment using photocatalytic technique: Case study yaakob village, sw sohag, Egypt. *J. Mater. Environ. Sci.* **2017**, *8*, 310–317.

75. Petroff, J.T.; Nguyen, A.H.; Porter, A.J.; Morales, F.D.; Kennedy, M.P.; Weinstein, D.; El Nazer, H.; McCulla, R.D. Enhanced photocatalytic dehalogenation of aryl halides by combined poly-p-phenylene (PPP) and TiO₂ photocatalysts. *J. Photochem. Photobiol. A Chem.* **2017**, *335*, 149–154. [CrossRef]

76. Zhao, C.; Pelaez, M.; Duan, X.; Deng, H.; O'Shea, K.; Fatta-Kassinos, D.; Dionysiou, D.D. Role of pH on photolytic and photocatalytic degradation of antibiotic oxytetracycline in aqueous solution under visible/solar light: Kinetics and mechanism studies. *Appl. Catal. B Environ.* **2013**, *134–135*, 83–92. [CrossRef]

77. Liu, Y.; Ao, Y.; Wang, C.; Wang, P. Enhanced photoelectrocatalytic performance of TiO₂ nanorod array under visible light irradiation: Synergistic effect of doping, heterojunction construction and cocatalyst deposition. *Inorg. Chem. Commun.* **2019**, *108*, 107521. [CrossRef]

78. Fagan, R.; McCormack, D.E.; Dionysiou, D.D.; Pillai, S.C. A review of solar and visible light active TiO₂ photocatalysis for treating bacteria, cyanotoxins and contaminants of emerging concern. *Mater. Sci. Semicond. Process.* **2016**, *42*, 2–14. [CrossRef]

79. Ito, Y.; Matsuda, K.; Kanemitsu, Y. Mechanism of photoluminescence enhancement in single semiconductor nanocrystals on metal surfaces. *Phys. Rev. B-Condens. Matter Mater. Phys.* **2007**, *75*, 033309. [CrossRef]

80. Nazir, M.; Aziz, M.I.; Ali, I.; Basit, M.A. Revealing antimicrobial and contrasting photocatalytic behavior of metal chalcogenide deposited P25-TiO2 nanoparticles. *Photonics Nanostructures-Fundam. Appl.* **2019**, *36*, 100721. [CrossRef]

81. Yang, H.; Long, Y.; Li, H.; Pan, S.; Liu, H.; Yang, J.; Hu, X. Carbon dots synthesized by hydrothermal process via sodium citrate and NH4HCO3 for sensitive detection of temperature and sunset yellow. *J. Colloid Interface Sci.* **2018**, *516*, 192–201. [CrossRef] [PubMed]

82. Aguedach, A.; Brosillon, S.; Morvan, J.; Lhadi, E.K. Photocatalytic degradation of azo-dyes reactive black 5 and reactive yellow 145 in water over a newly deposited titanium dioxide. *Appl. Catal. B Environ.* **2005**, *57*, 55–62. [CrossRef]

83. Monga, D.; Basu, S. Enhanced photocatalytic degradation of industrial dye by g-C3N4/TiO2 nanocomposite: Role of shape of TiO2. *Adv. Powder Technol.* **2019**, *30*, 1089–1098. [CrossRef]

84. Omidvar, H.; Sajjadnejad, M.; Mirzaei, K.; Sadeghian, Z.; Shirazi, S.; Mozafari, A.; Azadmehr, A. Characterisation of CNTs/TiO2 nano composites and investigation of composite's photo reactivity. *Int. J. Mater. Prod. Technol.* **2016**, *52*, 333–346. [CrossRef]

85. Yang, H.M.; Park, S.J. Effect of incorporation of multiwalled carbon nanotubes on photodegradation efficiency of mesoporous anatase TiO2 spheres. *Mater. Chem. Phys.* **2017**, *186*, 261–270. [CrossRef]

86. Alsharaeh, E.; Ahmed, F.; Arshi, N.; Alturki, M. Metal oxide nanophotocatalysts for water purification. In *Renewable Energy Technologies for Water Desalination*, 1st ed.; CRC Press: London, UK, 2017; pp. 57–72.

87. Arun Vargees, J.; FelixMarudai, J.; Monica, K.; Panchamoorthy, G. Application of Nano-Photocatalysts for Degradation and Disinfection of Wastewater. *J. Colloid Interface Sci.* **2012**, *366*, 135–140. [CrossRef]

88. Belver, C.; Bedia, J.; Gómez-Avilés, A.; Peñas-Garzón, M.; Rodriguez, J.J. Semiconductor Photocatalysis for Water Purification. Elsevier: New York, NY, USA, 2018; ISBN 9780128139271.

89. Weiss, C.; Carriere, M.; Fusco, L.; Fusco, L.; Capua, I.; Regla-Nava, J.A.; Pasquali, M.; Pasquali, M.; Pasquali, M.; Scott, J.A.; et al. Toward Nanotechnology-Enabled Approaches against the COVID-19 Pandemic. *ACS Nano* **2020**, *14*, 6383–6406. [CrossRef] [PubMed]

90. Sökmen, M.; Değerli, S.; Aslan, A. Photocatalytic disinfection of Giardia intestinalis and Acanthamoeba castellani cysts in water. *Exp. Parasitol.* **2008**, *119*, 44–48. [CrossRef]

91. Zheng, X.; Shen, Z.-P.; Cheng, C.; Shi, L.; Cheng, R.; Yuan, D. hai Photocatalytic disinfection performance in virus and virus/bacteria system by Cu-TiO2 nanofibers under visible light. *Environ. Pollut.* **2018**, *237*, 452–459. [CrossRef] [PubMed]

92. Wadhwa, S.; Mathur, A.; Pendurthi, R.; Singhal, U.; Khanuja, M.; Roy, S.S. Titania-based porous nanocomposites for potential environmental applications. *Bull. Mater. Sci.* **2020**, *43*, 47. [CrossRef]

93. Cheng, Y.W.; Chan, R.C.Y.; Wong, P.K. Disinfection of Legionella pneumophila by photocatalytic oxidation. *Water Res.* **2007**, *41*, 842–852. [CrossRef] [PubMed]

94. Etacheri, V.; Michlits, G.; Seery, M.K.; Hinder, S.J.; Pillai, S.C. A highly efficient TiO2-xCx nano-heterojunction photocatalyst for visible light induced antibacterial applications. *ACS Appl. Mater. Interfaces* **2013**, *5*, 1663–1672. [CrossRef]

95. Wei, H.; Banhe, Z.; Wuchun, C.; Dongling, Y.; ARAI, J.; Xiyun, Y. The inactivation effect of photocatalytic titanium apatite filter on SARS virus. *Sheng Wu Hua Xue Yu Sheng Wu Wu Li Jin Zhan* **2004**, *31*, 982–985.

96. Brugnera, M.F.; Miyata, M.; Zocolo, G.J.; Fujimura Leite, C.Q.; Boldrin Zanoni, M.V. A photoelectrocatalytic process that disinfects water contaminated with Mycobacterium kansasii and Mycobacterium avium. *Water Res.* **2013**, *47*, 6596–6605. [CrossRef] [PubMed]

97. Pan, Y.; Wang, Y.; Wu, S.; Chen, Y.; Zheng, X.; Zhang, N. One-pot synthesis of nitrogen-doped TiO2 with supported copper nanocrystalline for photocatalytic environment purification under household white led lamp. *Molecules* **2021**, *26*, 6221. [CrossRef]

98. Riaz, N.; Fen, D.A.C.S.; Khan, M.S.; Naz, S.; Sarwar, R.; Farooq, U.; Bustam, M.A.; Batiha, G.E.S.; El Azab, I.H.; Uddin, J.; et al. Iron-zinc co-doped titania nanocomposite: Photocatalytic and photobiocidal potential in combination with molecular docking studies. *Catalysts* **2021**, *11*, 1112. [CrossRef]

99. Koli, V.B.; Ke, S.-C.; Dodamani, A.G.; Deshmukh, S.P.; Kim, J.-S. Boron-Doped TiO2-CNT Nanocomposites with Improved Photocatalytic Efficiency toward Photodegradation of Toluene Gas and Photo-Inactivation of Escherichia coli. *Catalysts* **2020**, *10*, 632. [CrossRef]

100. Schneider, G.; Schweitzer, B.; Steinbach, A.; Pertics, B.Z.; Cox, A.; Kőrösi, L. Antimicrobial Efficacy and Spectrum of Phosphorous-Fluorine Co-Doped TiO2 Nanoparticles on the Foodborne Pathogenic Bacteria *Campylobacter jejuni*, *Salmonella* Typhimurium, Enterohaemorrhagic *E. coli*, *Yersinia enterocolitica*, *Shewanella putrefaciens*, *Listeria monocytogenes* and *Staphylococcus aureus*. *Foods* **2021**, *10*, 1786. [CrossRef] [PubMed]

101. Varnagiris, S.; Urbonavicius, M.; Sakalauskaite, S.; Demikyte, E.; Tuckute, S.; Lelis, M. Photocatalytic inactivation of salmonella typhimurium by floating carbon-doped TiO2 photocatalyst. *Materials* **2021**, *14*, 5681. [CrossRef]

102. Sikong, L.; Kongreong, B.; Kantachote, D.; Sutthisripok, W. Inactivation of salmonella typhi using Fe3+ doped TiO2/3SnO2 photocatalytic powders and films. *J. Nano Res.* **2010**, *12*, 89–97. [CrossRef]

103. Horovitz, I.; Avisar, D.; Luster, E.; Lozzi, L.; Luxbacher, T. MS2 bacteriophage inactivation using a N-doped TiO2-coated photocatalytic membrane reactor: Influence of water-quality parameters MS2 bacteriophage inactivation using a N-doped TiO2-coated photocatalytic membrane reactor: Influence of water-quality. *Chem. Eng. J.* **2018**, *354*, 995–1006. [CrossRef]

104. Daikoku, T.; Takemoto, M.; Yoshida, Y.; Okuda, T.; Takahashi, Y.; Ota, K.; Tokuoka, F.; Kawaguchi, A.T.; Shiraki, K. Decomposition of Organic Chemicals in the Air and Inactivation of Aerosol- Associated Influenza Infectivity by Photocatalysis. *Aerosol Air Qual. Res.* **2015**, *15*, 1469–1484. [CrossRef]
105. Woo, E.; Lee, H.; Hee, J.; Ha, J. Science of the Total Environment Photocatalytic inactivation of viral particles of human norovirus by Cu-doped TiO$_2$ non-woven fabric under UVA-LED wavelengths. *Sci. Total Environ.* **2020**, *749*, 141574. [CrossRef]